Fast Living-Body Localization Algorithm for MIMO Radar in Multi-path Environment

Dai Sasakawa, *Student Member, IEEE*
Naoki Honma, *Member, IEEE*
Takeshi Nakayama, Shoichi Iizuka *Non Member, IEEE*

***Abstract*—A fast living-body localization algorithm using time-differential channel suitable for multi-path environments is introduced. In this method, a time-differential channel is calculated from the difference among the observed channels that correspond to known biological activities such as respiration and heartbeat. The living-body locations are estimated by applying two-dimensional MUltiple SIgnal Classification (MUSIC) to the correlation matrix calculated from the time-differential channels. Experiments were carried out in an indoor environment, and the results show that the proposed localization algorithm could well estimate multiple device-free living-bodies simultaneously. The experimental results demonstrate that the locations of up to three persons could be estimated faster, within a few seconds, and more accurately than the conventional method. One, two or three targets yield 90% values of localization errors of 0.23 m, 0.41 m and 1.29 m, respectively.**

***Index Terms*—MIMO radar, DOA/DOD estimation, living-body localization, microwave sensors.**

I. Introduction

RECENTLY, the populations of many countries are aging rapidly. The increase in the number of elderly people is increasing the need for safety-monitoring systems that can detect people in distress due to events such as falls or sudden cardiopulmonary arrest. Conventional safety-monitoring systems include video cameras [1] or electrocardiography (ECG) [2]. However, the former can violate privacy, place heavy burdens on the monitoring system, and is provided only line-of-sight coverage. The latter forces the elderly to wear an instrument that can measure heartbeat, and places excessive physical and mental burdens on the user due to the direct and continuous wearing of the probe.

To avoid these problems, living-body localization methods that use microwave radar are being studied. The use of microwaves yields several key advances; privacy protection, ease of installation and use, and non-line-of-sight coverage. Accordingly, microwave radar can monitor all daily life areas and detect safety-related events such as falls. Two approaches have been investigated for human localization: Direction of Arrival (DOA) /Direction of Departure (DOD) - based Multiple-Input Multiple-Output (MIMO) radar systems [3][4] and TDOA (Time Difference of Arrival) estimation [5][6]. Unfortunately, the former cannot localize targets in multi-path environments because the wave reflected from the target suffers interference by the strong multi-path waves common in actual environments. Though the latter approach can quickly localize living-bodies by using Frequency-Modulated Continuous-Wave (FMCW) radar in a multi-path environment, this method requires wide bandwidth, 1.79 GHz (from 5.46 GHz to 7.25 GHz).

Object localization based on the MUltiple SIgnal Classification (MUSIC) method has been reported by Miwa et al. [7]. This system uses a low-frequency band, 250 MHz, and estimates the target location by using spherical-mode MUSIC to process the oscillating return signal. However, this method requires observation periods of over 10 seconds and the array aperture is comparable to the estimation distance because of the low frequency.

The authors have, for multi-path environments, proposed a living-body localization method that uses MIMO radar [8]-[10] based on DOA estimation using the Fast Fourier Transform (FFT) [11]. In this method, the fluctuating components created by the living-bodies is extracted from the Fourier-transformed virtual Single-Input Multiple-Output (SIMO) channel [3]. The target directions from the transmitting and receiving antennas are estimated by applying the MUSIC method to the fluctuating components. The target locations are taken to be the intersections of DOA (direction of arrival) and DOD (direction of departure). However, this method needs to observe the channel for several tens of seconds to accurately capture human activity information.

The authors have also proposed fast living-body direction estimation where the time-differential channel is used to attain rapid DOA estimation in multi-path environments [12]. This method uses SIMO radar and excludes undesired waves by taking the differences among the observed channels that correspond to cyclic human activities such as respiration and heartbeat. Though living-body direction can be estimated by applying the DOA estimation method to the time-differential channel, this antenna arrangement could not localize a target because only a single transmitting element was used. The proposal also could not estimate the directions of multiple targets because the rank of the correlation matrix is degenerated by the instantaneous subtraction of the observed channel.

This paper presents a fast living-body localization algorithm that uses the time-differential channel in multi-path environments. The proposed algorithm identifies the differences among observation times that correspond to cyclic human activities such as respiration and heartbeat. We define this calculated channel as the instantaneous time-differential channel. The living-body locations are estimated by applying two-dimensional MUSIC method [15] to the time-differential channel. This algorithm has an observation period that corresponds to one cycle of biological activity. Furthermore, its key

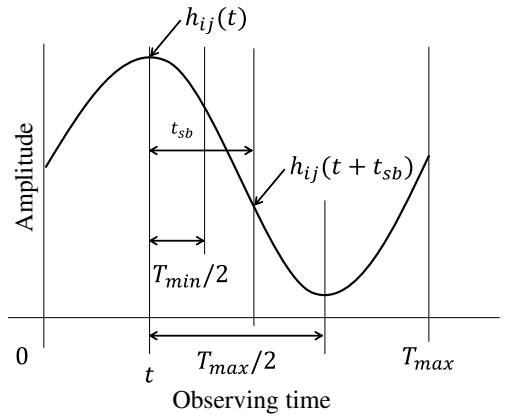

Fig. 1. Concept of biological signal.

feature is that this method does not require measurement of the static environment in advance, which is expected to yield immediate detection of the abnormal state of the target, as it utilizes biological activity including respiration and heartbeat. Moreover, the advantage of the proposed method is that the highly accurate localization is realized using the narrow band signal even with the multiple passive targets, i.e. device-free human-bodies. While our prior paper confirmed that time-differential channels are effective for localization by estimating the target location and trajectories [16], it did not address the estimation of multiple targets and no quantitative evaluation of estimation error was made. Therefore, this paper shows the theoretical foundation of the proposed method. Experiments carried out in an actual indoor environment demonstrate that the median value of localization error is better than 0.5 m.

II. Fast Living-body Localization Algorithm using Time-differential Channel

The authors previously proposed a living-body localization method that Fourier transforms the output of MIMO radar in multi-path environments [8]-[10]. However, this method has a problem in that channel measurements over several tens of seconds are needed to localize targets. In this section, the authors propose a fast living-body localization algorithm that treats time-differential channels in multi-path environments. The following explains the algorithm in detail.

This study assumes bistatic MIMO radar with an M_r element linear array receiver and an M_t element linear array transmitter. In a multi-path environment containing L persons, the $M_r \times M_t$ time-variant MIMO channel that is captured is expressed as,

$$\boldsymbol{H}(t) = \begin{pmatrix} h_{11}(t) & \dots & h_{1M_t}(t) \\ \vdots & \ddots & \vdots \\ h_{M_r1}(t) & \dots & h_{M_rM_t}(t) \end{pmatrix}, \quad (1)$$

where, h_{mn} is the complex channel response from the n-th transmitter element to the m-th receiver element, and t represents the observation time. $M_t \times M_r$ bistatic MIMO radar can be considered as $M_rM_t \times 1$ virtual SIMO radar[3]. Here, the observed $M_t \times M_r$ MIMO channel is converted into the $M_rM_t \times 1$ virtual SIMO channel,

$$\boldsymbol{h}(t) \quad = \quad [h_{11}(t), \cdots, h_{M_r1}(t), \cdots, h_{M_rM_t}(t)]^T, \quad (2)$$

where, $\{\cdot\}^T$ means transposition. Then, the observed channel includes desired components from targets and undesired components such as direct waves from transmitter to receiver, reflected waves from walls, furniture, and so on. In order to estimate living-body locations by DOA and DOD from the virtual SIMO channel, it is necessary to exclude the undesired waves.

The proposed method calculates the time-differential channel to exclude undesired waves. Fig. 1 shows the conceptual diagram of the received biological signal. The signal is fluctuated by biological activities such as respiration, heartbeat, and body motion. Here, the instantaneous time-differential channel is defined by the virtual SIMO channel at t subtracted from the channel after t_{sb}, and expressed by,

$$\boldsymbol{h}_{sb}(t, t_{sb}) \quad = \quad \boldsymbol{h}(t) - \boldsymbol{h}(t + t_{sb}). \quad (3)$$

The undesired components present in the observed channel are stationary in time. Therefore, the instantaneous time-differential channel excludes the undesired components, and the variation components created by the living-bodies are extracted.

First, we need to define the time difference t_{sb} that will accurately extract the variation components. We start by defining the maximum and minimum periods of the cyclic biological activities as T_{max} and T_{min}, respectively. In most cases, respiration is slower than or body motion so the maximum period T_{max} corresponds to respiration, and heartbeat or body motion corresponds to minimum period T_{min}. As shown in Fig. 1, the time difference t_{sb} is one half the cycle of biological activity when the gap between the received biological signal $\boldsymbol{h}(t)$ and $\boldsymbol{h}(t + t_{sb})$ is biggest. Therefore, the range of the time difference t_{sb} is defined as $T_{min}/2 \leq t_{sb} \leq T_{max}/2$. Also, the time-variant channel is observed for long enough to include one cycle of biological activity. Therefore, observing time t is defined as $0 \leq t \leq T_{max}/2$.

Here, the instantaneous correlation matrix using the time-differential channel $\boldsymbol{h}_{sb}(t, t_{sb})$ with observing time t and time difference t_{sb} is defined as,

$$\boldsymbol{R}(t, t_{sb}) = \boldsymbol{h}_{sb}(t, t_{sb})\boldsymbol{h}_{sb}(t, t_{sb})^H, \quad (4)$$

where, $\{\cdot\}^H$ means complex conjugate transposition. The rank of the instantaneous matrix $\boldsymbol{R}(t, t_{sb})$ is degenerate because it is extracted from an instantaneous time-differential channel. Therefore, we cannot estimate multiple target locations from the instantaneous correlation matrix. In order to recover eigenvalue rank, an averaged correlation matrix is calculated by averaging on both axes, the observing time and the time difference. This is expressed as,

$$\boldsymbol{R}_{ave} \quad = \quad \overline{\boldsymbol{R}(t, t_{sb})}$$

$$\big(0 \leq t \leq T_{max}/2, T_{min}/2 \leq t_{sb} \leq T_{max}/2\big), \quad (5)$$

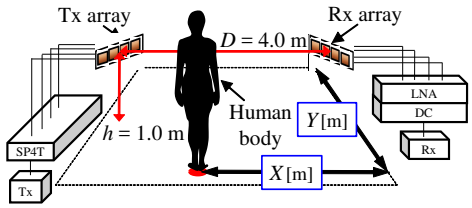

Fig. 2. Measurement setup.

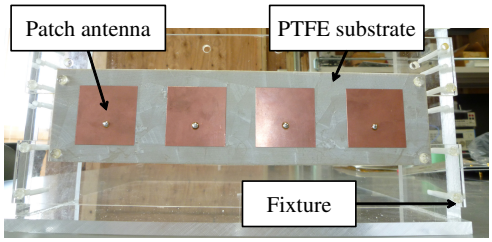

Fig. 3. Photo of array antenna.

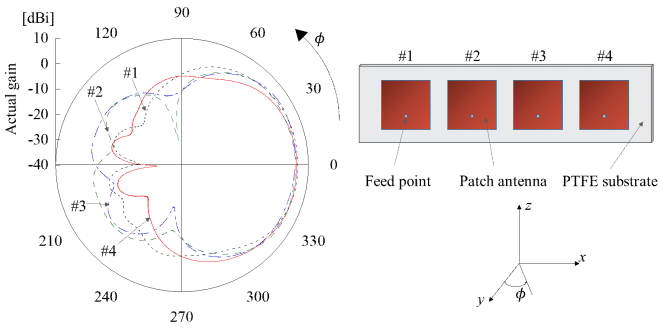

Fig. 4. Array element patterns of the patch array antenna.

where, $\overline{\{\cdot\}}$ is the averaging operator. In an actual measurement, the time-variant channel has a discrete variable, so the averaged correlation matrix is expressed as,

$$\boldsymbol{R}_{ave} = \frac{1}{MN}\sum_{m=0}^{M}\sum_{n=0}^{N}\boldsymbol{R}(mT_s, nT_s + \frac{T_{min}}{2}), \quad (6)$$

$$M = \frac{T_{max}}{2T_s} + 1, \quad (7)$$

$$N = \frac{(T_{max} - T_{min})}{2T_s} + 1, \quad (8)$$

where, T_s means the snapshot acquisition period. By eigenvalue decomposition, the averaged correlation matrix $\boldsymbol{R}_{ave}$ is given by,

$$\boldsymbol{R}_{ave} = \boldsymbol{U}\boldsymbol{\Lambda}\boldsymbol{U}^H, \quad (9)$$

$$\boldsymbol{U} = [\boldsymbol{u}_1, ..., \boldsymbol{u}_L, ..., \boldsymbol{u}_{M_rM_t}], \quad (10)$$

$$\boldsymbol{\Lambda} = \mathrm{diag}([\lambda_1, ..., \lambda_L, ..., \lambda_{M_rM_t}]), \quad (11)$$

where, $\boldsymbol{U}$ and $\boldsymbol{\Lambda}$ represent the eigenvector and the diagonal matrix representing eigenvalues, respectively. At this time, eigenvalues $\boldsymbol{\Lambda}$ are related as follows,

$$\lambda_1 \geq \cdots \geq \lambda_L > \lambda_{L+1} = \cdots = \lambda_{M_rM_t} = \sigma_f^2, \quad (12)$$

where, σ_f^2 represents the expected value of the energy of the channel fluctuation component caused by the influence of noise. The noise eigenvalue, $[\lambda_{L+1}, ..., \lambda_{M_rM_t}]$, corresponding to eigenvector, $[\boldsymbol{u}_{L+1}, ..., \boldsymbol{u}_{M_rM_t}]$, is expressed as $\boldsymbol{U}_N$. Here, we use the two-dimensional MUSIC algorithm with spherical mode vector; the original MUSIC method [13] [14] extended to cover the 2D domain [15]. The MUSIC spectrum peaks are found by applying the 2D-MUSIC method with its virtual MIMO steering vector to the averaged correlation matrix, and the spectrum peaks represent estimated target locations. The proposed method has the theoretical upper limit of the number of the target, which is determined by the number of the receiving and transmitting antenna elements. In this case, the limit is $(M_r \times M_t - 1)$, which corresponds to the number of the eigenvalues minus one.

III. Measurement Conditions and Experimental Environment

Fig. 2 shows the measurement setup. The experiments used a 4×4 bistatic MIMO configuration. As shown in Fig. 2, a Single-Pole 4 Throw (SP4T) switch was used at the transmitting side. Though the exact observation time was not the same for all elements in the MIMO channel matrix, the time differences among the elements are so short compared to the vital activity that they are ignored. A continuous wave (CW) signal at 2.47125 GHz was used, and transmitted power at the antennas was set to 7.0 dBm. At the receiver side, received signals were input to a down-converter (DC) unit by way of a Low-Noise Amplifier (LNA) unit. The down-converted baseband signals were received by a data-acquisition unit (DAQ). The receiver and transmitter used four horizontally arranged patch antennas with half wavelength element spacing. Fig. 3 shows a photo of the array antenna used in these measurements. An array antenna used a PTFE substrate, and its thickness, width (including four antenna elements) and height were 1.6, 255 and 60 mm, respectively. The array's center was set to $h = 1.0$ m, the trunk height of the subjects. The straight line distance between transmitting and receiving antennas was set to 4.0 m. The receiver and the transmitter faced the center of the room.

Fig. 4 shows the measured array element patterns of the patch array antenna that consists of four elements. The tested area is covered within the half-power beam-width because the antennas (receiver and transmitter) faced the center of the room.

Measurements were made for various numbers of subjects in different locations. The frequency range most strongly influenced by human respiration runs from 0.6 to 3.3 Hz, while the frequency range most strongly influenced by human heart rate runs from 0.33 to 0.5 Hz [17]. Therefore, in this study, time difference t_{sb} was set to 0.14 [s] $\leq t_{sb} \leq$ 1.71 [s]. Prior to measurements, the observation channels were measured for 3.29 seconds. After that we evaluate the effective observation time by the localization accuracy. The snapshot acquisition period of the MIMO channels was set to 1/7 of a second. The transmission components of S parameters were

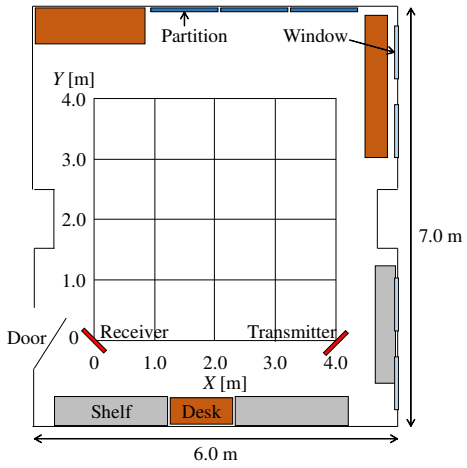

Fig. 5. Experimental environment.

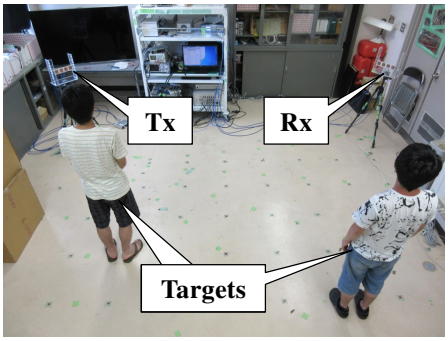

Fig. 6. Photo of two targets in the experimental environment.

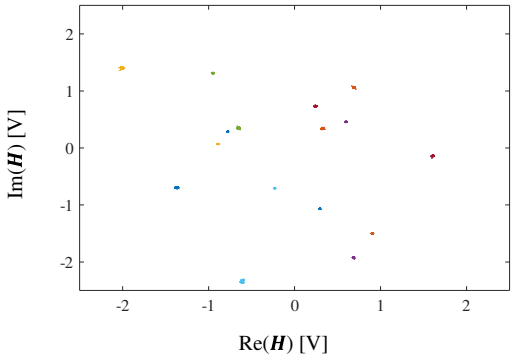

Fig. 7. Static channel response in the complex plane.

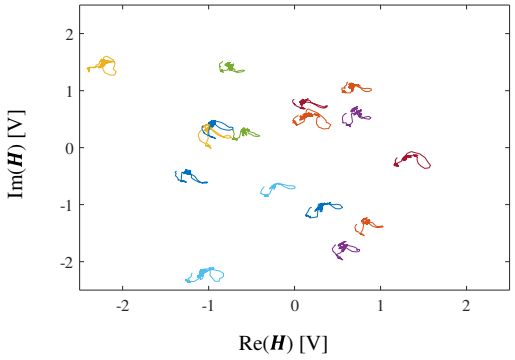

Fig. 8. Channel response with one person; complex plane representation.

used as the propagation channel. The number of targets, L, was determined following the MUSIC method.

Fig. 5 shows the experimental environment. The environment was a cluttered room containing furniture and fixtures such as tables and shelves along the walls. The room had concrete walls and its width, depth, and height were 7.0, 6.0, and 2.7 m, respectively. One side of the room had are four windows. Fig. 6 shows a photo of a time-variant channel measurement. When the channel was observed, there was only target, and the targets stood facing the wall against which the antenna were set.

The array antenna had to be calibrated because of the have phase error created by the Radio Frequency (RF) front-end. The target or targets stood at predetermined places and measurements were made. The calibration value was determined by applying the SIMO radar calibration method [18] extended for MIMO radar.

As the accuracy metric, this study uses acceptable error. Because human body width can be approximated as 0.5 m, 90-th percentile estimation error better than 0.5 m is considered to be acceptable.

IV. Measurement Results

Fig. 7 and Fig. 8 show examples of the time-variant channel response (complex plane representation) without/with a living-body, respectively. In Fig. 7, the received signals show almost no variation because the propagation environment was not changed. In comparison with the static channel response, the time-variant channel with a living-body of Fig. 8 exhibits change because the living-body disturbs the transmission environment. Additionally, the variation demonstrates the periodicity of the biological activities.

Fig. 9 shows an observed time-variant channel response with and without one target. The channel response in this figure is $h_{11}(t)$ of the measured $M_r \times M_t$ time-variant MIMO channel matrix. The power of h_{11} with the living-body is lowered by the fading in the multi-path environment. The amplitude of the raw channel coefficient does not represent the signal strength of the vital sign, i.e. the channel is the sum of the paths via the living- and non-living bodies. Again, the presence of the living-body clearly perturbs the observed channel, and the variation by the vital sign periodically vibrates h_{11}.

Fig. 10 shows an example of the time-differential channel calculated from the measured time-variant channel in Fig. 9. In this figure, the horizontal axis represents the observing time difference t_{sb}, and the time-differential channel plots the difference between the preliminary observation time, 3.29 sec, and observing time t. This figure shows that the time-differential channel with living-body exhibits a periodic variation corresponding to biological activity with a peak at $t = 1.29$ sec. The net signal-to-noise ratio (SNR) is the ratio of

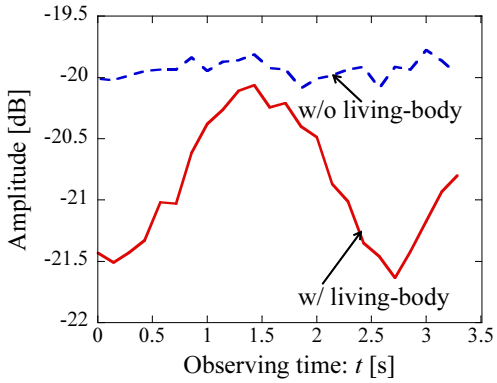

Fig. 9. Example of the time-variant channel.

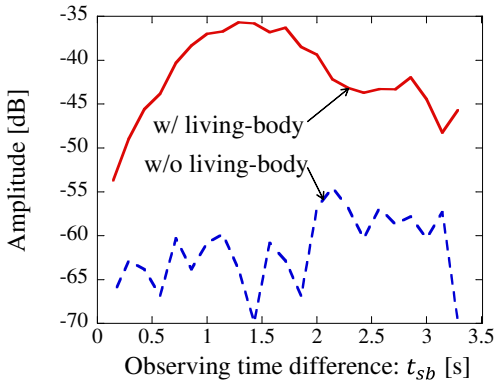

Fig. 10. Example of the time-differential channel.

the vital sign strength over the noise power. As for the time-differential channel, only the variant component (vital sign) is extracted from the raw channel. In Fig. 10, the amplitude of the time-differential channel with the target represents the reflected power from the target, which corresponds to the fluctuation of the variation of the body surface by the vital activity. Meanwhile, the time-differential channel without living-body shows no regularity. The intensity of the transition of the time-differential channel shows the net SNR of the measured data because the waveforms with and without a living-body represent the vital sign and noise. This result shows that the SNR is sufficient to observe the vital sign of the living-body. Therefore, biological information can be extracted from the observed channel by calculating the time-differential channel.

Fig. 11 shows an example of the MUSIC spectrum for living-body localization when there is one person at ($X = 2.0$ m, $Y = 2.0$ m). In this figure, the circle and diamond represent the actual target location and the spectrum peak (i.e. estimated location), respectively. This figure confirms that the estimated location lies close to the actual location of the target.

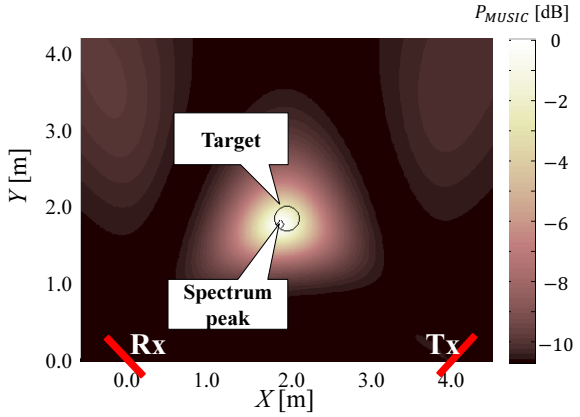

Fig. 11. Example of the MUSIC spectrum for localization when one target was present.

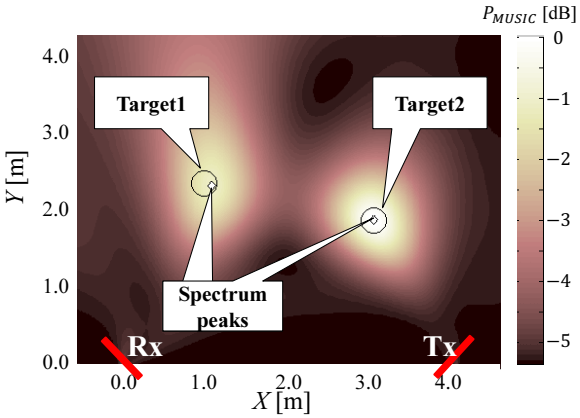

Fig. 12. Example of the MUSIC spectrum for localization when two targets were present.

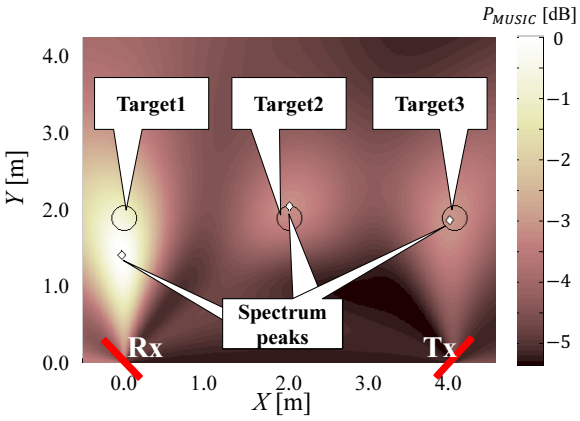

Fig. 13. Example of the MUSIC spectrum for localization when three targets were present.

Therefore, the proposed method can well estimate living-body location in multi-path environments.

Fig. 12 shows an example of the MUSIC spectrum for

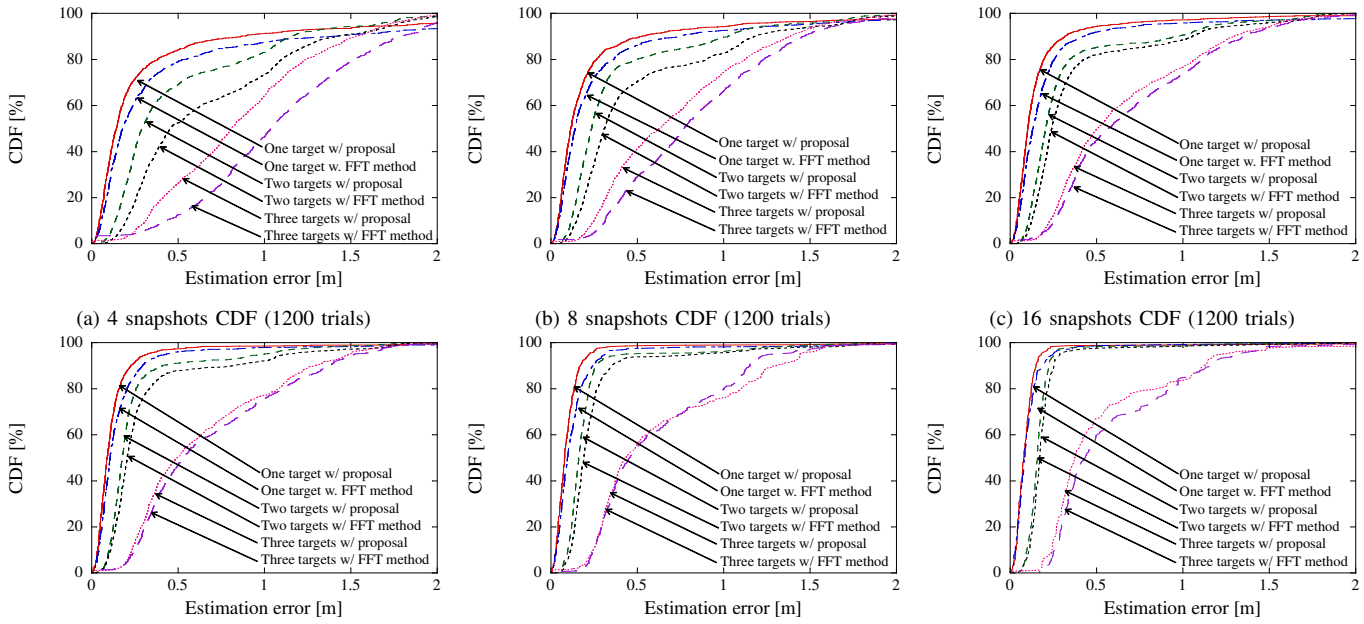

(a) 4 snapshots CDF (1200 trials)
(b) 8 snapshots CDF (1200 trials)
(c) 16 snapshots CDF (1200 trials)
(d) 32 snapshots CDF (1000 trials)
(e) 64 snapshots CDF (500 trials)
(f) 128 snapshots CDF (200 trials)

Fig. 14. CDF of estimation error for each snapshot.

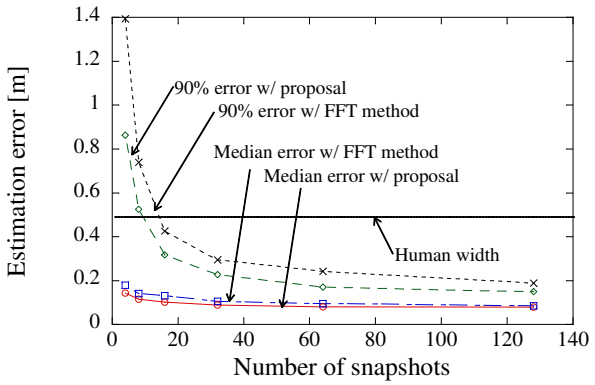

Fig. 15. Median and 90% error versus the number of snapshots with one target.

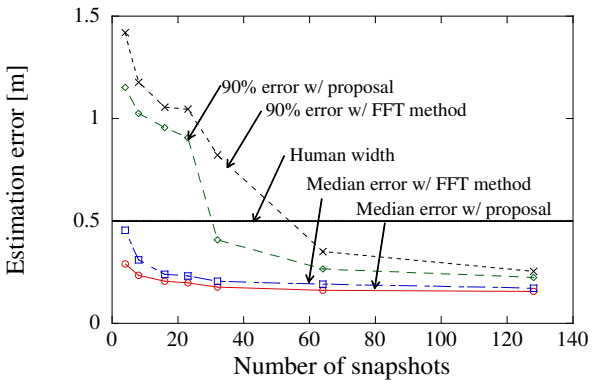

Fig. 16. Median and 90% error versus the number of snapshots with two targets.

localization with two people. Target1 and target2 stood at ($X = 1.0$ m, $Y = 2.5$ m) and ($X = 3.0$ m, $Y = 2.0$ m), respectively. In this figure, the spectrum peaks appear within each target circle (centered on actual location). This result confirms that the proposed method can estimate the locations of multiple targets by recovering eigenvalue rank.

Fig. 13 shows an example of the localization result for three people. Target1, target2, and target3 stood at ($X = 0.0$ m, $Y = 2.0$ m), ($X = 2.0$ m, $Y = 2.0$ m), and ($X = 4.0$ m, $Y = 2.0$ m), respectively. In this figure, the spectrum peaks of target2 and target3 lie within the target circle, while the peak of target1 is close to target1's circle. Thus, the estimation error of target1 is about 0.5 m. This confirms that the proposed method can localize even three targets simultaneously. We discuss the accuracy of estimation later using a statistical characterization.

Next, we evaluate the estimation error by the observation time (i.e. the number of snapshots). In the proposed algorithm, when the total observation time t_{ob} was less than $T_{max} = 3.3$ [s], the observing time t and the time difference t_{sb} were defined as 0 [s] $\leq t \leq t_{ob} - T_{max}/2$ [s].

Fig. 14 shows the cumulative distribution function (CDF) of the localization error estimated by the proposed method and a conventional method (FFT technique [10]) with one, two and three targets, respectively. The localization error was defined by the Euclidean distance between the actual target locations and the estimated positions. The estimation error means the averaged error of each target localization error when there were two and three subjects. All plots in Fig. 14 show that the proposal yields better estimation accuracy than the conventional method regardless of the number of targets and snapshots. However, it is confirmed that estimation accuracy is low with just a few snapshots. Fig. 14(a) shows the CDF of the estimation error with 4 snapshots (i.e. the observation time is 0.43 seconds). The 90% values of the proposed method are

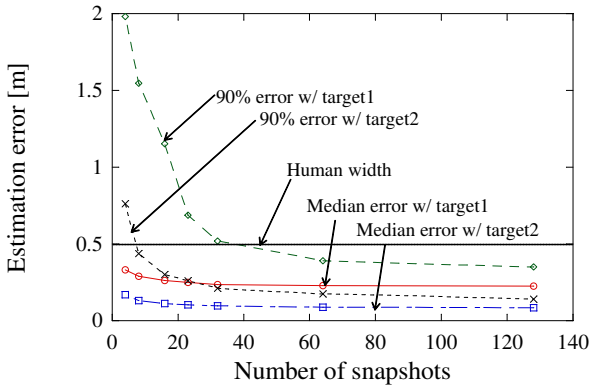

Fig. 17. Median and 90% error values of each target versus the number of snapshots with two targets: proposed method.

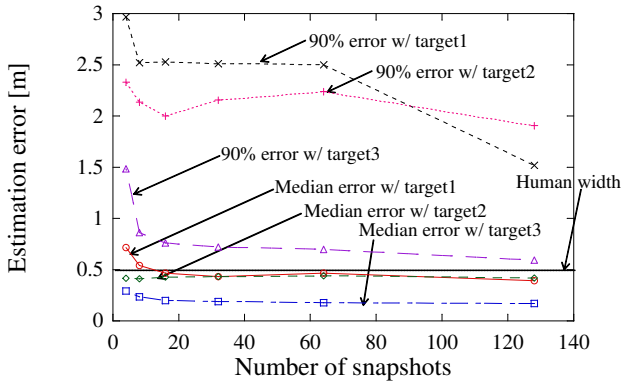

Fig. 19. Median and 90% error values of each target versus the number of snapshots with three target: proposed method.

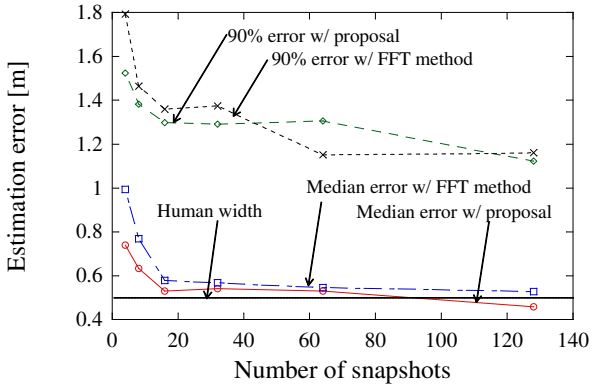

Fig. 18. Median and 90% error versus the number of snapshots with three targets.

0.86 m, 1.15 m and 1.52 m for one, two and three targets, respectively. These values exceed our definition of acceptable error. Fig. 14(b) shows the CDF of the estimation error with 8 snapshots; observation time is 1.00 second. In this figure, the 90% values are 0.52 m, 1.03 m, and 1.38 m for one, two and three targets, respectively. While these values also exceed the acceptable error, they are clearly better than the 4 snapshot case. Fig. 14(c) shows the CDF of the estimation error with 16 snapshots; observation time is 2.14 seconds. In Fig. 14(c), the 90% values of the proposed method are 0.32 m, 0.96 m and 1.30 m for one, two and three targets, respectively. here, the 90% value with one target does satisfy the acceptable error. We mention the factor of the estimation error with multiple targets later. Fig. 14(d) shows the CDF of the estimation error with 32 snapshots,; observation time is 4.43 seconds. The 90% values of the proposed method are 0.23 m, 0.41 m and 1.29 m for one, two and three targets, respectively. The 90% value of the proposed method with one or two subjects is lower than the acceptable error. On the other hand, since the 90% value of the conventional method is 0.82 m, i.e., over the acceptable error, the FFT method requires longer observation time. In Fig. 14(e) and (f), the observation times are 9.00 and 18.14 seconds, respectively. Observing the channel for longer periods improves the accuracy. Note that the proposal and conventional method yield similar results in Fig. 14(f). In particular, the estimation accuracies with three subjects were still inadequate.

Fig. 15 shows the median and 90% value of the localization error versus the number of snapshots with one target. In this figure, though the 90% values of the proposal and the conventional method satisfy the acceptable error at the same time, the former has error of 0.32 m which is superior to that of the latter, 0.43 m. It can be seen that the proposed method yields a 0.11 m improvement in localization accuracy with 16 snapshots. Also, all median values of the estimation error results are below 0.2 m.

Fig. 16 shows the median and 90% value of the averaged localization error versus the number of snapshots with two subjects. The median averaged error with the proposed and FFT method were within the acceptable error. Of particular interest, the proposal attained median errors below 0.3 m for each snapshot number examined. The largest accuracy difference between the proposal and conventional method (90% value) is 0.41 m with 32 snapshots ($= 4.43$ [s]). With two subjects, the 90% value of the FFT method exceeds the acceptable error, while the 90% value of the proposal is better than 0.5 m.

Fig. 17 shows the median and 90% errors of the proposed method for each target. The channel was measured with target1 and target2 standing at $(X, Y) = (1.0, 2.5)$ [m] and $(X, Y) = (3.0, 2.0)$ [m], respectively. In this figure, the localization results of target2 are more accurate than those of target1 for all observation time, which is reasonable given that target2 was closer to the transmitter.

Fig. 18 shows, for the proposed and conventional method, the median and 90% averaged localization error versus snapshot number with three targets. Though the median and 90% error values improve as snapshot number is increased to 16, the median values exceed the acceptable error. The estimation accuracy basically saturates beyond 16 snapshots, and so can be considered as the limit of three subject localization.

Fig. 19 shows the median and 90% error of the proposed method for each of three targets in isolation. Target1, target2, and target3 stood at $(X, Y) = (0.0, 2.0)$ [m], $(X, Y) = (2.0, 2.0)$ [m] and $(X, Y) = (4.0, 2.0)$ [m], respectively. In this figure, the median localization error of each target

satisfies the acceptable error at 16 snapshots. The difference between those results and the median error in Fig. 18 is the simultaneous presence of the targets. The proposal can localize one or two targets accurately, but is weak when there are three subjects simultaneously. It can be seen that paucity in the degree of freedom available for the estimation is the cause of the degraded localization accuracy. The degree of freedom is four in this experiment as we used 4by4 MIMO radar. Because the proposed and conventional method used MUSIC [13], only one degree of freedom was used when localizing three targets. A simple solution is to increase the number of MIMO antenna elements. Regarding the estimation results of target3, though the accuracy was short of the acceptable error, localization was far more precise than for the other targets as it was closest to the transmitter.

Fig. 20 shows the tracking result when the target was approaching the transmitter. The 8×8 MIMO configuration was used for this demonstration. The receiver and transmitter have eight horizontally arranged patch antennas that are just extended array of the configuration shown in the Fig. 3. The antenna thickness, width, and height were 1.6, 480 and 60 mm, respectively. The element spacing was half wavelength. The distance between the transmitter and the receiver was set to 8.0 m. A CW signal at 2.47 GHz was used, too. In this trial, the time window length for detecting the target was 2.56 seconds. The period of taking snapshots of the MIMO channels per second was set to 50 Hz. During the measurement, the target walked straight at the speed of 0.7 m/s from $(0, 8)$ [m] to $(7, 1)$ [m]. In this figure, the solid line indicates the actual movement line, and the circles represent the locations of the target estimated by the proposed algorithm. In this figure, 94 points were estimated. At the start position $(X, Y) = (0, 8)$ [m], there were circle like movement in the estimated locations because the subject did not start walking at this moment. Also, there were three outliers from the actual movement line in the results, and the maximum error was 6.36 m. Meanwhile, most of the estimated error from the actual movement line is within the acceptable error (91 points /94 points=96.8%). The median value of the estimated error from the movement line was 0.18 m, and the averaged error was 0.35 m. This result shows that the proposed method can successfully estimate the trajectory of the walking target in the conference room.

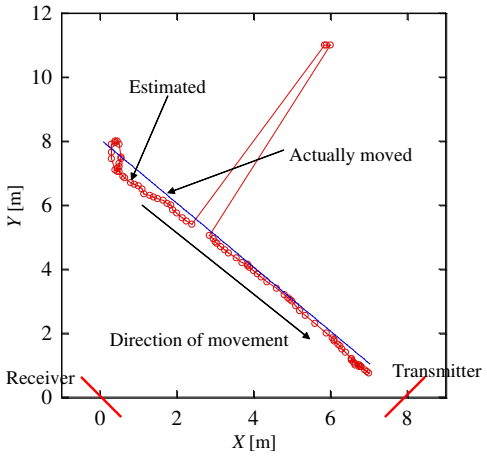

Fig. 20. Tracking result of the walking target; the target moved straightly from (0, 8) [m] to (7, 1) [m] at the speed of 0.7 m/s.

V. Conclusion

This paper proposed a fast living-body localization algorithm that treats time-differential channels in multi-path environments. A time-differential channel is calculated as the difference among the observed channels generated by biological activities; the differencing eliminates constant unwanted components such as direct waves, reflected waves from wall and so on. The proposed algorithm can also localize multiple targets by recovering eigenvalue rank by averaging in terms of observation duration and time difference. We estimate target locations by applying the 2-dimensional MUSIC method to the averaged correlation matrix by casting the system as a virtual SIMO array. Experiments were carried out in an indoor environment. The results showed that with one subject, 2.14 s measurement periods yielded localization error below 0.5 m. In the case of two targets, 4.43 s measurement periods yielded a 90% value of the averaged estimation error under the acceptable error limit. For three targets, though the 90% value exceeded the acceptable error, the median error of each target was less than 0.5 m. Moreover, in case of multiple subjects, the location of the target closest to the transmitter was detected most accurately. These results confirm that the proposed method can accurately localize living-bodies within few seconds in multi-path environments.

References

[1] H. Seki and Y. Hori, "Detection of abnormal action using image sequence for monitoring system of aged people," The transactions of IEEJ. D, A publication of Industry Applications Society 122(2), pp.182-188, Feb. 2002.

[2] T. Martin, E. Jovanov, D. Raskovic, "Issues in wearable computing for medical monitoring applications: a case study of a wearable ECG monitoring device," International Symposium on Wearable Computers (ISWC'00), pp.43-49, Oct. 2000.

[3] J. Li, P. Stoica, MIMO radar signal processing, A John Wiley & Sons, inc., 2009.

[4] H. Yan, J. Li, G. Liao, "Multitarget identification and localization using bistatic MIMO radar systems", EURASIP J. Adv. in Signal Process., vol. 2008, no. ID 283483, 2008.

[5] F. Adib, Z. Kabelac, D. Katabi, and RC. Miller, "3d tracking via body radio reflections," 11th USENIX Symposium on Networked Systems Design and Implementation (NSDI'14), Vol. 14, pp.317-329, Apr. 2014.

[6] F. Adib, Z. Kabelac, and Katabi, "Multi-person motion tracking via RF body reflections," Computer Science and Artificial Intelligence Laboratory Technical Report, MIT-CSAIL-TR-2014-008, April 26, 2014.

[7] T. Miwa, S. Ogiwara, and Y. Yamakoshi, "Localization of living-bodies using single-frequency multistatic Doppler radar system," IEICE Trans. Commun., vol.E92-B, No.7, pp.2468-2476, Jul. 2009.

[8] D. Sasakawa, K. Konno, N. Honma, K. Nishimori, N. Takemura, and T. Mitsui, "Localizing living body using bistatic MIMO radar in multi-path environment," 8th European Conference on Antennas and Propagation (EUCAP 2014), Electric Proc. of EuCAP 2014, pp.3863-3867, Apr. 2014.

[9] Keita Konno, Naoki Honma, Dai Sasakawa, Yoshitaka Tsunekawa, Kentaro Nishimori, and Nobuyasu Takemura, "Localizing Multiple Target Using Bistatic MIMO Radar in Multi-path Environment," 2014 IEEE International Workshop on Electromagnetics: Applications and Student Innovation Competition (iWEM 2014), Vol.2, pp. 90-91, Aug. 2014.

[10] K. Konno, N. Honma, D. Sasaskawa, K. Nishimori, N. Takemura, T. Mitsui, and Y. Tsunekawa, "Estimating living-body location using bistatic MIMO radar in multi-path environment," IEICE Transactions on Communications, Vol. E98-B, No.11, pp. 2314-2321, Nov. 2015.

[11] Keita Konno, Masaki Nango, Naoki Honma, Kentaro Nishimori, Nobuyasu Takemura, and Tsutomu Mitsui, "Experimental evaluation of estimating living-body direction using array antenna for multipath environment," IEEE Antennas Wireless Propag. Lett., Vol. 13, pp.718-721, Apr. 2014.
[12] D. Sasakawa, K. Konno, N. Honma, K. Nishimori, N. Takemura, and T. Mitsui, "Fast estimation algorithm for living body radar," 2014 International Symposium on Antennas and Propagation (ISAP 2014), FR3D, pp. 583-584, Dec. 2014.
[13] R. Schmidt, "Multiple emitter location and signal parameter estimation," IEEE Transactions on Antennas and Propagation, Vol. 34, Issue 3, pp. 276 - 280, Mar. 1986.
[14] C. Plapous, J. Cheng, E. Taillefer, A. Hirata, and T. Ohira, "Reactance domain MUSIC algorithm for electronically steerable parasitic array radiator," IEEE Transactions on Antennas and Propagation, Vol. 52, Issue 12, pp. 3257 - 3264, Dec. 2004.
[15] M. L. Bencheikh, Y. Wang, and H. He, "Polynomial root finding technique for joint DOA DOD estimation in bistatic MIMO radar", Signal Processing, Vol. 90, Issue 9, pp. 2723-2730, Sep. 2010.
[16] D. Sasakawa, N. Honma, K. Nishimori, T. Nakayama and S. Iizuka, "Evaluation of fast human localization and tracking using MIMO radar in multi-path environment," 27th Annual IEEE International Symposium on Personal, indoor and Mobile Radio Communications, WeB8.4, pp.1148-1153, Sep. 2016.
[17] J. M. Park, D. H. Choi and S. O. Park, "Wireless vital signal detection systems and its applications at 1.9 GHz and 10 GHz," 2003 IEEE/ Antennas and Propagation Society International Symposium, vol. 4, pp. 747-750, Jun. 2003.
[18] D. Sasakawa, K. Konno, N. Honma, K. Nishimori, N. Takemura, and T. Mitsui, "Antenna array calibration for living body radar," IEEE Antennas Wireless Propag. Lett., vol.15, pp.246-249, Feb. 2016.

Dai Sasakawa received the B.E. and M.E. degree in electrical and electronic engineering from Iwate University, Morioka, Japan in 2014 and 2016, respectively. He is currently in the Ph.D. program in Iwate University. He received the Young Engineers Award from the IEICE of Japan in 2017. His current research interest is MIMO systems for human monitoring.

Naoki Honma received the B.E., M.E., and Ph.D. degrees in electrical engineering from Tohoku University, Sendai, Japan in 1996, 1998, and 2005, respectively. In 1998, he joined the NTT Radio Communication Systems Laboratories, Nippon Telegraph and Telephone Corporation (NTT), in Japan. He is now working for Iwate University. He received the Young Engineers Award from the IEICE of Japan in 2003, the APMC Best Paper Award in 2003, the Best Paper Award of IEICE Communication Society in 2006, and 2014 Asia-Pacific Microwave Conference Prize in 2014, respectively. His current research interest is MIMO system and its applications. He is a member of IEEE.

Takeshi Nakayama received the B.E., M.E. degrees in Department of Opt-electronic & Mechanical Engineering, Faculty of Engineering from Shizuoka University, Shizuoka, Japan in 1994, 1996, respectively. In 1996, he joined the Multimedia Development Center, Matsushita Electric Industrial Co., Ltd. (Panasonic Corporation), in Japan. He is now working for Panasonic Corporation. His current research interest is MIMO system and its applications.

Shoichi Iizuka received the B.E. and M.E. degrees in information science and technology from Osaka University, Osaka, Japan in 2013 and 2015, respectively. He joined Appliances Company, Panasonic Corporation in 2015. His current research interest is living-body radar system and its applications. He is a member of Information Processing Society of Japan.